Article

Cell Reports

Structural Constraints Determine the Glycosylation of HIV-1 Envelope Trimers

Graphical Abstract

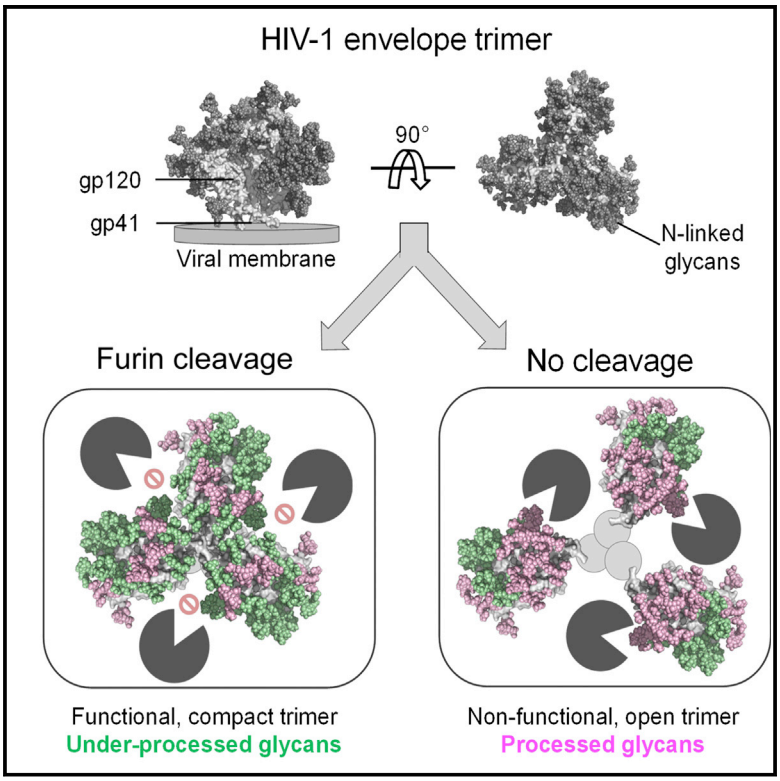

Authors

Laura K. Pritchard, Snezana Vasiljevic, Gabriel Ozorowski, ..., Andrew B. Ward, John P. Moore, Max Crispin

Correspondence

max.crispin@bioch.ox.ac.uk

In Brief

The HIV-1 envelope spike is the major target for vaccine design. Pritchard et al. show that the quaternary structure of this trimeric glycoprotein determines the processing of its extensive glycan coat. Structural constraints inhibit cellular processing, leaving a largely homogeneous oligomannose population that can be targeted by the immune system.

Highlights

- Native-like, cleaved HIV-1 Env mimetics are dominated by underprocessed *N*-glycans
- In contrast, non-native uncleaved trimers undergo greater glycan processing
- The Env quaternary structure dictates the degree of glycan processing that can occur
- The abundance of homogeneous oligomannose glycans is promising for vaccine design

Pritchard et al., 2015, Cell Reports *11*, 1604–1613
June 16, 2015
http://dx.doi.org/10.1016/j.celrep.2015.05.017

OPEN ACCESS
CellPress

Cell Reports
Article

Structural Constraints Determine the Glycosylation of HIV-1 Envelope Trimers

Laura K. Pritchard,[1,10] Snezana Vasiljevic,[1,10] Gabriel Ozorowski,[2] Gemma E. Seabright,[1] Albert Cupo,[3] Rajesh Ringe,[3] Helen J. Kim,[2] Rogier W. Sanders,[3,4] Katie J. Doores,[5] Dennis R. Burton,[6,7,8,9] Ian A. Wilson,[2] Andrew B. Ward,[2] John P. Moore,[3] and Max Crispin[1,*]

[1]Oxford Glycobiology Institute, Department of Biochemistry, University of Oxford, South Parks Road, Oxford OX1 3QU, UK
[2]Department of Integrative Structural and Computational Biology, IAVI Neutralizing Antibody Center and the collaboration for AIDS Vaccine Discovery, Center for HIV/AIDS Vaccine Immunology and Immunogen Discovery, Skaggs Institute for Chemical Biology, The Scripps Research Institute, 10550 North Torrey Pines Road, La Jolla, CA 92037, USA
[3]Department of Microbiology and Immunology, Weill Cornell Medical College, New York, New York, NY 10021, USA
[4]Laboratory of Experimental Virology, Department of Medical Microbiology, Center for Infection and Immunity Amsterdam (CINIMA), Academic Medical Center of the University of Amsterdam, 1105 AZ Amsterdam, the Netherlands
[5]King's College London School of Medicine at Guy's, King's and St. Thomas' Hospitals, Guy's Hospital, Great Maze Pond, London SE1 9RT, UK
[6]Department of Immunology and Microbial Science, The Scripps Research Institute, La Jolla, CA 92037, USA
[7]International AIDS Vaccine Initiative Neutralizing Antibody Center, The Scripps Research Institute, La Jolla, CA 92037, USA
[8]Center for HIV/AIDS Vaccine Immunology and Immunogen Discovery, The Scripps Research Institute, La Jolla, CA 92037, USA
[9]Ragon Institute of Massachusetts General Hospital, Massachusetts Institute of Technology and Harvard University, Boston, MA 02142, USA
[10]Co-first author
*Correspondence: max.crispin@bioch.ox.ac.uk
http://dx.doi.org/10.1016/j.celrep.2015.05.017

SUMMARY

A highly glycosylated, trimeric envelope glycoprotein (Env) mediates HIV-1 cell entry. The high density and heterogeneity of the glycans shield Env from recognition by the immune system, but paradoxically, many potent broadly neutralizing antibodies (bNAbs) recognize epitopes involving this glycan shield. To better understand Env glycosylation and its role in bNAb recognition, we characterized a soluble, cleaved recombinant trimer (BG505 SOSIP.664) that is a close structural and antigenic mimic of native Env. Large, unprocessed oligomannose-type structures ($Man_{8-9}GlcNAc_2$) are notably prevalent on the gp120 components of the trimer, irrespective of the mammalian cell expression system or the bNAb used for affinity purification. In contrast, gp41 subunits carry more highly processed glycans. The glycans on uncleaved, non-native oligomeric gp140 proteins are also highly processed. A homogeneous, oligomannose-dominated glycan profile is therefore a hallmark of a native Env conformation and a potential Achilles' heel that can be exploited for bNAb recognition and vaccine design.

INTRODUCTION

The HIV-1 envelope glycoprotein (Env) is a trimer of gp120-gp41 heterodimers that mediates viral entry into host cells (Liu et al., 2008). As the sole target of broadly neutralizing antibodies (bNAbs) (Hessell et al., 2009; Mascola et al., 2000; Moldt et al., 2012), it is likely that an effective prophylactic vaccine against HIV-1 will include a recombinant protein based on the Env trimer. Given that the trimer is approximately half carbohydrate by mass (Lasky et al., 1986), an important consideration for the antigenicity, and perhaps also the immunogenicity, of a recombinant version is the extent to which its glycans resemble and function like those on viral Env. The enormous relevance of glycans in HIV-1 vaccine design is underscored by the isolation of numerous distinct families of potent bNAbs whose binding is dependent on Env glycans (Blattner et al., 2014; Falkowska et al., 2014; Garces et al., 2014; Huang et al., 2014; Kong et al., 2013; McLellan et al., 2011; Mouquet et al., 2012; Pancera et al., 2013; Pejchal et al., 2011; Scharf et al., 2014; Walker et al., 2009, 2011).

Studies on monomeric gp120 proteins have consistently identified two major subgroups of glycan structures: underprocessed oligomannose and processed complex glycans (Bonomelli et al., 2011; Doores et al., 2010; Go et al., 2013; Leonard et al., 1990; Raska et al., 2010). The underprocessed glycans contain multiple terminal mannose sugars (typically five to nine, referred to as $Man_5GlcNAc_2$ to $Man_9GlcNAc_2$). Underprocessed glycans are, therefore, often referred to as "high-mannose" or "oligomannose" glycans (we prefer hereon to use the latter term). During processing in the endoplasmic reticulum (ER) and early Golgi apparatus, α-mannosidase enzymes remove a subset of mannose moieties before various other carbohydrate components are added, predominantly in the medial and late Golgi, to create complex glycans. Whether an oligomannose glycan is then further modified is not a random event; it is determined by the spatial location and accessibility of the glycan site on the folded protein. The dominant factor is most probably whether

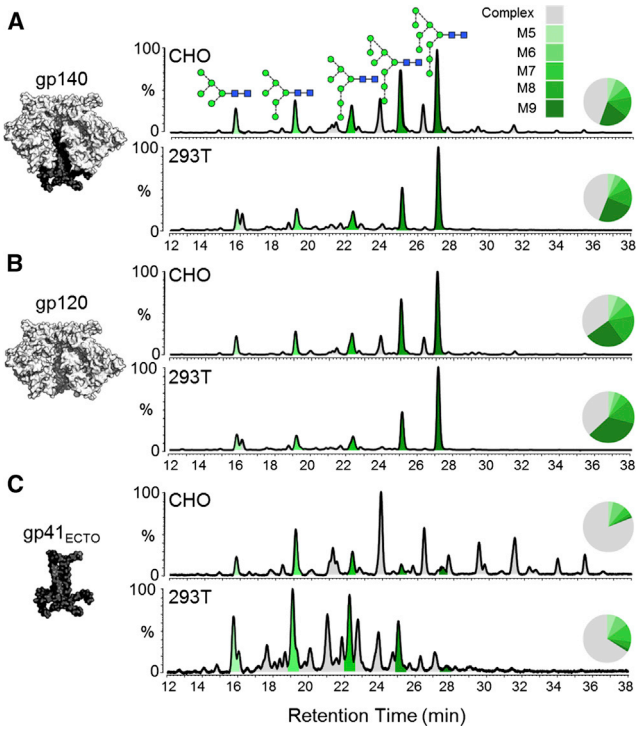

Figure 1. Comparison of Glycosylation Patterns of BG505 SOSIP.664 Trimers Produced in CHO and 293T Cells

(A–C) HILIC-UPLC spectra of fluorescently labeled N-linked glycans isolated from (A) the entire trimeric gp120/gp41$_{ECTO}$ complex (gp140) and the (B) gp120 and (C) gp41$_{ECTO}$ subunits of BG505 SOSIP.664 trimers. The subunits analyzed in each case are illustrated on the left. Trimers were purified by 2G12-affinity chromatography followed by SEC. The gp140 band was extracted from a non-reducing SDS-PAGE gel, while the gp120 and gp41$_{ECTO}$ bands were resolved by SDS-PAGE under reducing conditions. The glycan contents of proteins extracted from the bands were analyzed. Peaks corresponding to oligomannose glycans (M5-M9; $Man_{5-9}GlcNAc_2$) are colored in shades of green; the remaining peaks (gray) correspond to complex and hybrid-type glycans. Peak areas (as a percentage of total glycans) are illustrated in the associated pie charts. Glycan structures are represented according to the color scheme established by the Consortium for Functional Glycomics (http://www.functionalglycomics.org/). The SOSIP.664 construct contains the following mutations: a T332N mutation to introduce the 332 glycosylation site, cysteines at 501 and 605 form a disulphide bridge to covalently link the gp120 and gp41$_{ECTO}$ subunits, replacement of the gp120 furin cleavage site (REKR) with a hexa-arginine (R6) sequence to promote furin cleavage, an I559P mutation to stabilize the gp41$_{ECTO}$ subunits in the prefusion form, and deletion of the MPER region at residue 664 to reduce aggregation.

α-mannosidases can gain access to their substrates since unprocessed glycans are sterically shielded by other glycans and/or the protein backbone. The unprocessed glycans in HIV-1 Env tend to be clustered in the "intrinsic mannose patch" (IMP), thereby creating a large exposed surface of conserved glycans that can be targeted by bNAbs and that contains multiple overlapping epitopes (Calarese et al., 2003; Garces et al., 2014; Kong et al., 2013; Mouquet et al., 2012; Murin et al., 2014; Sanders et al., 2002; Scanlan et al., 2002; Walker et al., 2009, 2011).

Glycan characterization of native, virion-derived trimers remains a challenge due to difficulties in obtaining a sample sufficient for analysis, due in large part to the very limited numbers of Env proteins on the viral surface. Previous studies have confirmed the presence of an IMP on virion-derived gp120; however, further investigation, including characterization of gp41 glycosylation, was not possible (Bonomelli et al., 2011; Doores et al., 2010). In this study, we have investigated the glycosylation of a highly purified, recombinant, soluble Env trimer, BG505 SOSIP.664. These trimers closely mimic the structure and antigenicity of native, virion-associated Env, and their high-resolution EM and crystal structures have been determined (Julien et al., 2013; Lyumkis et al., 2013; Pancera et al., 2014; Sanders et al., 2013). We have quantified the glycan composition of BG505 SOSIP.664 trimers expressed in several cell types and purified in different ways, in comparison with other forms of recombinant Env that are being considered as candidate HIV-1 vaccines. Our results show that gp120 subunits from BG505 SOSIP.664 trimers contain a homogeneous glycan profile that is characterized by a high abundance of the largest oligomannose-type structures, $Man_{8-9}GlcNAc_2$. In contrast, glycosylation of gp41 is reflected by cell-specific processing and dominated by complex-type glycans. Analysis of uncleaved BG505 SOSIP.664 glycoproteins, as well as uncleaved gp140 oligomers from BG505 and other genotypes, revealed a much higher degree of processing, which could be correlated with more open and irregular Env configurations that, by extrapolation, reduce the structural constraints on the relevant carbohydrate processing enzymes. Thus, the quaternary structure of HIV-1 Env is, in itself, an important parameter in determining how native trimers are glycosylated.

RESULTS

Protein-Directed Glycosylation of gp120 Subunits of Env Trimers

BG505 SOSIP.664 gp140 trimers were expressed in stably transfected Chinese hamster ovary (CHO) or 293T cells and purified using a 2G12 bNAb-affinity column followed by size exclusion chromatography (SEC), as previously described (Chung et al., 2014). The CHO and 293T cell-derived trimers, purified by the same method, had similar apparent molecular weights (Figure S1). When resolved by SDS-PAGE in the presence of the reducing agent DTT, the gp120 and gp41$_{ECTO}$ domains were fully separated, indicating that the gp140 proteins had been appropriately cleaved by furin during expression (Figure S1).

The N-linked glycans were released from SDS-PAGE gel bands by protein *N*-glycosidase F (PNGase F) digestion. The gp140 band was derived from a non-reduced SDS-PAGE gel, and the gp120 and gp41$_{ECTO}$ bands from a reduced gel. Isolated glycans were fluorescently labeled with 2-aminobenzoic acid (2-AA) and analyzed by hydrophilic interaction liquid chromatography-ultra performance liquid chromatography (HILIC-UPLC) (Figure 1). The peaks in the HILIC-UPLC profiles were assigned by sequential digestion of the labeled glycans with a panel of exoglycosidases (Figure S2; Table S1). The overall profiles of the BG505 SOSIP.664 trimers from CHO and 293T cells were very similar, with both containing a large population of oligomannose glycans (Figure 1A). Integration of the chromatograms revealed that oligomannose glycans accounted for 55% and 56% of the

Table 1. Abundances of Oligomannose Glycans in Different Env Proteins

Env Protein	Producer Cell	Affinity Purification Scheme	Abundance (% of Total Glycans)					
			M5[a]	M6	M7	M8	M9	Total
gp120 BG505 from Cleaved Trimers								
SOSIP.664	CHO	PGT151	5	7	8	18	27	66
SOSIP.664	CHO	PGT145	5	7	8	17	27	65
SOSIP.664	CHO	2G12	6	7	9	18	25	65
SOSIP.664	293T	2G12	4	4	6	15	34	63
SOSIP.664	293F	2G12	8	5	8	19	20	60
SOSIP.664	293F	PGT151	9	5	8	24	25	71
$gp41_{ECTO}$ BG505 from Cleaved Trimers								
SOSIP.664	CHO	2G12	3	8	5	2	1	19
SOSIP.664	293T	2G12	6	9	12	5	2	34
gp140 from Cleaved and Uncleaved Trimers[b]								
SOSIP.664[c]	CHO	2G12	6	8	8	14	20	55
SOSIP.664[c]	293T	2G12	5	5	8	13	25	56
BG505 WT.SEKS[d]	293T	2G12	6	5	8	12	11	42
CZA97.012[d]	293T	Ni^{2+}-NTA	10	4	7	7	3	30
CN54[d]	CHO	5F3	7	4	6	6	3	27
UG37[d]	CHO	5F3	9	4	5	10	14	42

[a]Mx refers to $Man_xGlcNAc_2$ glycans.
[b]Glycan profiles for gp140 constructs include contributions from both gp120 and $gp41_{ECTO}$ domains.
[c]Cleaved trimer.
[d]Uncleaved trimer.

total glycan population of the CHO and 293T-derived trimers, respectively (Table 1). $Man_8GlcNAc_2$ and $Man_9GlcNAc_2$ forms were particularly abundant, together representing 34% and 38% of the CHO and 293T-derived glycan pools, respectively.

Separation of the trimers into their constitutive subunits revealed that glycans from gp120 accounted for the majority of the overall gp140 profile, which is expected because 72 of the total 84 potential glycosylation sites on BG505 gp140 are located on the three gp120 subunits. The gp120 subunits from CHO and 293T cell-derived BG505 SOSIP.664 trimers contained 65% and 63% oligomannose glycans, respectively (Figure 1B; Table 1), with a comparable value (60%) for trimers expressed in 293F cells (Figure S3; Table S2). $Man_8GlcNAc_2$ and $Man_9GlcNAc_2$ together accounted for up to 49% of total glycan content (Figure S3; Tables 1 and S2). In contrast, oligomannose glycans were much less abundant on the $gp41_{ECTO}$ subunits (19% and 34% for CHO and 293T cell-derived trimers, respectively). The presence of a large population of complex-type glycans on the $gp41_{ECTO}$ subunits revealed the impact of the producer cell on glycosylation, with CHO cells generating more sialylated structures than 293T cells (Figures 1C and S2; Table S2).

Thus, the two subunits of the trimer are processed differently, with gp120 (60%–65%) having a higher oligomannose content than $gp41_{ECTO}$ (19%–34%). A likely explanation is that processing enzymes face greater restrictions when accessing gp120 because the local glycan density is so much greater compared with $gp41_{ECTO}$. Analysis of a crystal structure of the BG505 SOSIP.664 trimer (Pancera et al., 2014) reveals that the 72 gp120 glycosylation sites give rise to an average density of one per ~1,000 $Å^2$ surface area; for the 12 predicted gp41 glycosylation sites, the corresponding value is one per ~2,500 $Å^2$. Whether such differential processing and the resulting glycan composition differences are important for the function of the two subunits is not yet known.

Significantly, membrane-associated, cleaved (but non-SOSIP stabilized) BG505 EnvΔCT trimers, extracted from the cell membrane via PGT151 bNAb affinity purification (Blattner et al., 2014), were also highly enriched for oligomannose glycans and had a highly similar glycan profile to the comparable BG505 SOSIP.664 preparation (Figure S4). The similarity between the glycan content of soluble and membrane-extracted Env trimers therefore implies that the membrane does not confer additional constraints on glycan processing and that the design and methods used to create soluble SOSIP.664 trimers do not significantly impact the resulting glycosylation.

The Trimer Glycan Signature Is Independent of Glycan-Specific bNAb Purification

Glycan-dependent bNAbs differ in their specificities for glycan structures. We therefore sought to determine whether affinity purification via a 2G12 column had affected the glycan profile of the BG505 SOSIP.664 trimers analyzed above, by purifying the trimers in different ways. While 2G12 is selective for terminal Manα1→2Man on oligomannose glycans (Sanders et al., 2002; Scanlan et al., 2002), the PGT145 and PGT151 epitopes include complex glycans on the gp120 trimer apex and on $gp41_{ECTO}$, respectively (Blattner et al., 2014; Falkowska et al., 2014; McLellan et al., 2011). Moreover, PGT145 and PGT151 recognize quaternary structure-dependent epitopes that are present only on fully native trimers (Blattner et al., 2014; Falkowska et al.,

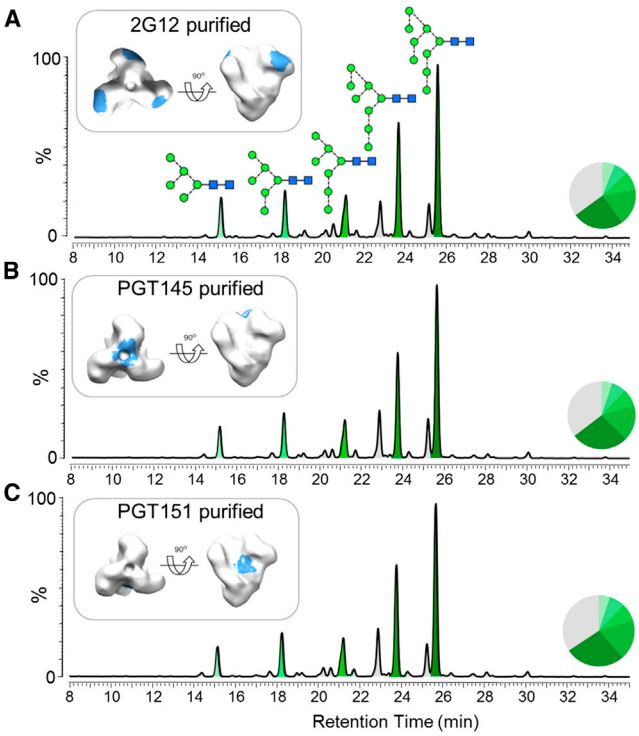

Figure 2. Glycan Profiles of BG505 SOSIP.664 Trimers following bNAb Affinity Purification

(A–C) CHO cell-derived trimers were purified by bNAb affinity chromatography using 2G12, PGT145 or PGT151, followed by SEC. Glycans isolated from reducing SDS-PAGE gel bands containing cleaved gp120 subunits were analyzed by HILIC-UPLC. The various bNAb epitopes are colored light blue on an EM reconstruction on the left. Peaks corresponding to oligomannose glycans are colored in shades of green, and the corresponding peak areas are illustrated in the associated pie charts, as in Figure 1. See also Figure S3.

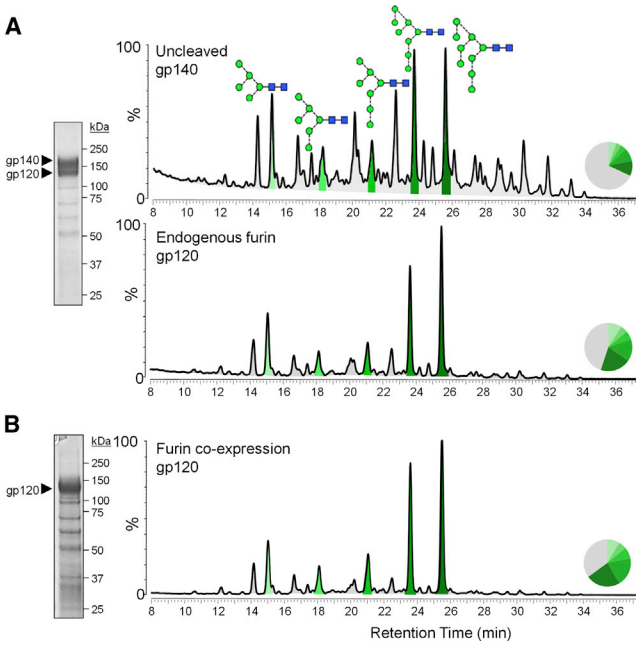

Figure 3. Effect of Proteolytic Cleavage on Env Glycan Processing

His-tagged BG505 SOSIP.664 trimers were expressed in 293F cells with and without furin co-expression and purified by Ni^{2+}-NTA affinity chromatography.

(A) Reducing SDS-PAGE of trimers expressed without furin, and the resulting HILIC-UPLC glycan profiles derived from gel bands corresponding to uncleaved gp140 (top) and cleaved gp120 (bottom).

(B) Reducing SDS-PAGE of the same trimers but co-expressed with furin, and the corresponding HILIC-UPLC glycan profiles derived from the band corresponding to cleaved gp120. Peaks corresponding to oligomannose glycans are colored in shades of green, and the corresponding peak areas are illustrated in the associated pie charts, as in Figure 1. SDS-PAGE analysis (both panels) reveals a minor population of low molecular weight contaminants.

2014; McLellan et al., 2011; Pugach et al., 2015). We found that trimers purified using PGT145, PGT151, and 2G12, in each case followed by SEC, had almost identical glycosylation profiles (Figure 2). The same finding was made when a His-tagged BG505 SOSIP.664 trimer was expressed in 293F cells and affinity purified using various bNAbs (2G12, PGT151, PGT145, PG9, and b12), after earlier Ni^{2+}-affinity chromatography and SEC purification (Figure S3; Table S2). Thus, irrespective of the bNAb used, the affinity-purified trimers had a very similar proportion of oligomannose glycans (60%–71%). The additional bNAb affinity purification step had little impact on the glycosylation profiles of the Ni^{2+}/SEC-purified BG505 SOSIP.664 trimers, which had a level of oligomannose glycans comparable to that found after a bNAb affinity purification step (Figure S3; Table S2).

The above findings strongly suggest that the observed dominance of large oligomannose glycoforms is an integral feature of the BG505 SOSIP.664 trimers, irrespective of the cell type used for expression (CHO, 293T, 293F). Moreover, as bNAbs with divergent glycan specificities (2G12, PGT151, PGT145, PG9) or with less glycan-dependent epitopes (b12) all recognize (i.e., purify) trimers that bear essentially indistinguishable glycan profiles, the trimer population must be highly homogeneous and consistently folded into a native conformation. Similar results from His-tag purification (i.e., glycan independent) support this conclusion.

Uncleaved Trimers Undergo Greater Levels of Glycan Processing

An alternative approach to making soluble gp140 immunogens is to eliminate the cleavage site between the gp120 and $gp41_{ECTO}$ subunits (Go et al., 2014; Kovacs et al., 2012; Ringe et al., 2013). The influence of furin cleavage on Env glycosylation is unknown. To assess whether this design difference affects glycan processing, we expressed His-tagged BG505 SOSIP.664 Env proteins without co-transfecting the furin protease. Endogenous furin is not sufficiently abundant to process all trimers transiting through the secretory pathway. Thus, both uncleaved (i.e., gp140 band) and cleaved (gp120 band) Env species were observed when SDS-PAGE was carried out under reducing conditions (Figure 3A). Comparison of the glycan composition of the gp140 and gp120 bands revealed remarkable differences; the gp140 band contained a much greater content of processed glycans than the gp120. The discrepancy was substantially greater than could be accounted for by the $gp41_{ECTO}$ subunit, which is present in the gp140 band but not the gp120 band (Figure 3A).

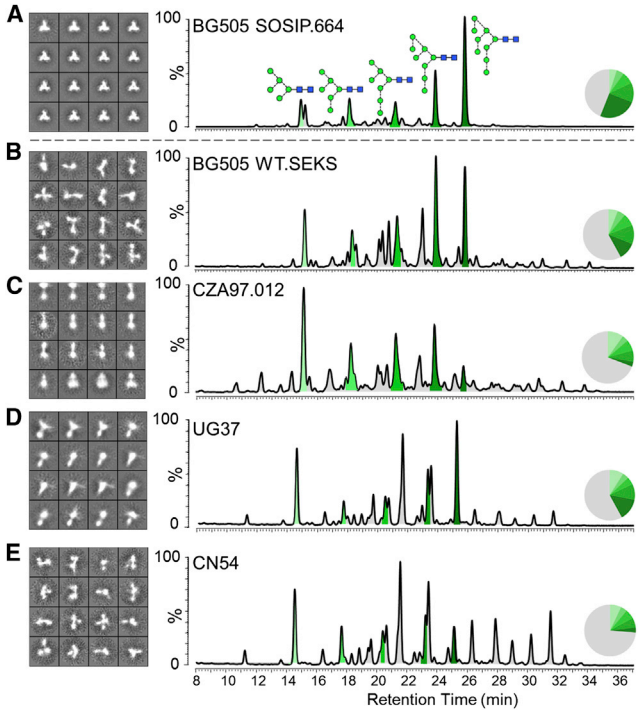

Figure 4. Disordered Configurations of Uncleaved gp140s Are Associated with Higher Levels of Glycan Processing

(A) HILIC-UPLC glycan data and 2D class averages from negative stain EM analysis are shown for BG505 SOSIP.664 trimers expressed in 293T cells and purified using 2G12-affinity chromatography followed by SEC. The UPLC chromatogram is reproduced from Figure 1A to facilitate data comparison.

(B) Uncleaved BG505 WT.SEKS gp140 expressed in 293T cells and purified by 2G12 affinity chromatography followed by SEC. Quantitation of the complete datasets shows that native-like, regular, and compact trimers constitute >90% of the images of the BG505 SOSIP.664 proteins. In contrast, <5% of the uncleaved BG505 WT.SEKS proteins are in native-like form, where the predominant images represent disordered, splayed out trimers.

(C–E) The same is also true of (C) uncleaved, His-tagged CZA97.012 gp140 proteins produced in 293T cells and purified by Ni^{2+}-NTA affinity chromatography followed by SEC; (D) uncleaved UG37 gp140; (E) uncleaved CN54 gp140 proteins (the latter two purchased from Polymun Scientific). Peaks corresponding to oligomannose glycans are colored in shades of green, and the corresponding peak areas are illustrated in the associated pie charts, as in Figure 1.

When furin was co-expressed with the same His-tagged BG505 SOSIP.664 construct, all the trimers were fully cleaved (Figure 3B). The glycan profile of the resulting SDS-PAGE gp120 band was highly similar to the corresponding band derived when endogenous furin cleaved only a subset of the trimers. Thus, co-transfecting furin with SOSIP.664 trimers does not adversely affect trimer glycosylation and, in fact, emulated natural cleavage. Moreover, cleavage by furin, whether endogenous or transfected, is sufficient to create a distinct oligomannose glycoform.

The Env Quaternary Structure Correlates with the Degree of Glycan Processing

To investigate why cleaved and uncleaved BG505 SOSIP.664 gp140s have such different glycan compositions, we used negative stain electron microscopy (EM) to visualize their configurations (Figure 4). The fully cleaved BG505 SOSIP.664 proteins form regular, homogeneous trimers with a characteristic propeller-like appearance (Figure 4A), which is consistent with previous studies (Chung et al., 2014; Ringe et al., 2013). The bNAb used for affinity purification did not affect the appearance of these trimers (data not shown). For comparison, we used the BG505 WT.SEKS gp140 protein, which has an identical sequence to the BG505 SOSIP.664 construct except that the furin cleavage site is inactivated (RRRRRR to SEKS) and the stabilizing SOSIP mutations are not included (Ringe et al., 2013). Similar to the observations of the uncleaved BG505 SOSIP.664 subpopulation (see above), the glycans on the uncleaved BG505 WT.SEKS gp140 were more highly processed than on their cleaved counterparts; oligomannose structures accounted for only 42% of the total glycan population, with $Man_8GlcNAc_2$ and $Man_9GlcNAc_2$ accounting for just 23% (Figure 4B; Table 1). When viewed by EM, the uncleaved BG505 WT.SEKS gp140 glycoproteins adopted irregular, non-native, and heterogeneous configurations in which the gp120 subunits were frequently splayed out (Figure 4B). These images are in marked contrast to the closed forms of the cleaved BG505 SOSIP.664 trimers and are consistent with previous studies of several other uncleaved gp140 proteins (Georgiev et al., 2015; Moscoso et al., 2014; Ringe et al., 2013; Tran et al., 2014).

A similar correlation between quaternary structure and glycan profile was also observed when analyzing further vaccine-relevant gp140 glycoproteins from different clades. The CZA97.012 protein derives from a subtype C sequence and has been studied in multiple immunization and other experiments (Go et al., 2014; Kovacs et al., 2012; Nkolola et al., 2010). Like the BG505 WT.SEKS gp140, it has a knocked-out cleavage site, but also includes foldon domains near the C-termini of the $gp41_{ECTO}$ subunits to artificially drive oligomerization (Go et al., 2014; Kovacs et al., 2012; Nkolola et al., 2010). The CZA97.012 gp140 was expressed in 293T cells and purified via its C-terminal His-tag followed by SEC, as previously described (Chung et al., 2014). The glycan composition of the SEC fraction corresponding to a protein with three gp120 and three $gp41_{ECTO}$ subunits was then determined (Figure 4C). This gp140 population contained only 30% oligomannose, with just 10% of the glycans in $Man_8GlcNAc_2$ or $Man_9GlcNAc_2$ form. Once again, the EM analysis revealed that most of these gp140s adopt a splayed-open conformation, with only a small fraction of particles (<10%) having a more compact appearance (Figure 4C). Similar EM results were also observed with two other uncleaved, foldon-containing glycoproteins, CN54 gp140 (clade C) and UG37 gp140 (clade A), which have also been investigated as candidate immunogens (Lewis et al., 2011, 2014; Schiffner et al., 2013). These gp140s were also predominantly irregularly shaped (Figures 4D and 4E), as described previously (Ringe et al., 2013). The observed disorder of the CN54 and UG37 gp140s again correlated with a high degree of glycan processing, the oligomannose content being 27% and 42%, respectively (Figures 4D and 4E; Table 1).

DISCUSSION

Oligomannose glycans, which are co-translationally added to glycoproteins, are typically efficiently processed to complex

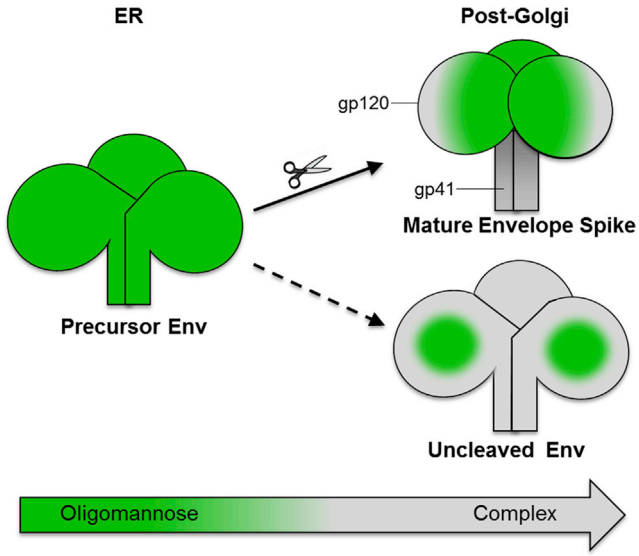

Figure 5. Env Cleavage Induces Highly Homogeneous Glycoforms Dominated by Oligomannose Glycans

Env is synthesized as a gp160 precursor in the ER, and oligomannose-type glycans are incorporated at glycosylation sequons: Asn-X-Ser/Thr (where X is any amino acid except Pro). As glycoproteins pass through the secretory pathway, they are exposed to α-mannosidases and other glycan processing enzymes, which normally convert oligomannose-type glycans (green) to complex-type glycans (gray). The quaternary structure of Env dictates how well processing enzymes can access the glycans on gp120. Cleaved Env exhibits a compact quaternary structure that prevents trimming by ER and Golgi α-mannosidases and is thus secreted as an oligomannose-dominated glycoform. In contrast, uncleaved Env has a more open and irregular structure that facilitates easier access by processing enzymes, leading to conversion of the majority of the oligomannose glycans to more complex-type structures. However, high glycan density on the outer domain of gp120 creates a region that is largely protected from α-mannosidase trimming, known as the IMP, which is present on both cleaved and uncleaved Env. Gp41 is more accessible to processing enzymes than gp120 and is dominated by complex-type glycosylation.

structures. The presence of oligomannose-type glycans on mature, native HIV-1 Env glycoproteins represents a divergence from this default pathway of "self" glycosylation and provides a potential window for immune recognition. Indeed, many potent bNAbs are glycan reactive (Blattner et al., 2014; Falkowska et al., 2014; Garces et al., 2014; Huang et al., 2014; Kong et al., 2013; McLellan et al., 2011; Mouquet et al., 2012; Pancera et al., 2013; Pejchal et al., 2011; Sanders et al., 2002; Scanlan et al., 2002; Scharf et al., 2014; Walker et al., 2009, 2011). The first described, 2G12, binds only to the terminal Manα1→2Man moieties of oligomannose glycans (Scanlan et al., 2002), while bNAbs such as the PGT series involve contacts with both glycans and protein (Blattner et al., 2014; Falkowska et al., 2014; Garces et al., 2014; Huang et al., 2014; Kong et al., 2013; McLellan et al., 2011; Mouquet et al., 2012; Pancera et al., 2013; Pejchal et al., 2011; Scharf et al., 2014; Walker et al., 2009, 2011). Overall, there is now widespread appreciation that vaccine candidates intended to induce bNAbs should have a glycan profile that mimics what is present on native Env trimers (Bonomelli et al., 2011; Burton et al., 2012; Crispin and Bowden, 2013; Doores et al., 2010; Dunlop et al., 2010).

BG505 SOSIP.664 trimers are highly stable and homogeneous, have native-like antigenic properties, and resemble viral Env when viewed by negative stain EM (Ringe et al., 2013; Sanders et al., 2013; Yasmeen et al., 2014). Although their EM and crystal structures have been determined, it was not possible to define the processing state of the glycans from the density maps (Julien et al., 2013; Lyumkis et al., 2013; Pancera et al., 2014). Here, we found that the gp120 subunits of the same SOSIP.664 trimers have a large oligomannose content, consistent with previous reports of virion-derived Env (Bonomelli et al., 2011; Doores et al., 2010). The distribution of oligomannose glycans throughout the $Man_{5-9}GlcNAc_2$ series was particularly notable, with $Man_8GlcNAc_2$ and $Man_9GlcNAc_2$ structures accounting for up to half of the glycan population. Presumably, their existence reflects protection from α-mannosidase processing that arises through the stabilization and conformational restrictions created by a network of glycan-glycan interactions that extend across the gp120 subunits of the trimer. These structural constraints are the primary determinant of Env glycosylation, and they create a reproducible glycan profile irrespective of the producer cell. In contrast, the lack of such constraints on the $gp41_{ECTO}$ subunits results in a greater dependency on the producer cell in determining the final glycan profile. The low abundance of oligomannose structures observed on $gp41_{ECTO}$ subunits here is consistent with the previously reported resistance of virion-derived trimeric gp41 to Endo H processing (Crooks et al., 2011).

Further support for structure-driven glycan processing on the native trimer comes from analysis of uncleaved gp140 proteins. EM images of these proteins generally show three separated gp120 subunits dangling from a central $gp41_{ECTO}$ moiety to which they remain tethered by the uncleaved inter-subunit linkage (Georgiev et al., 2015; Moscoso et al., 2014; Ringe et al., 2013; Tran et al., 2014), a conclusion strongly supported by hydrogen deuterium exchange-mass spectrometry (HDX-MS) and surface plasmon resonance (SPR) data (Guttman et al., 2014; Ringe et al., 2013; Yasmeen et al., 2014). The EM images of uncleaved gp140s shown here are entirely consistent, with irregularly shaped forms predominating. These more open configurations are reflected in their glycosylation profiles, which display a high degree of processing; in particular, there is a markedly lower abundance of $Man_8GlcNAc_2$ and $Man_9GlcNAc_2$ structures. A prior report of the highly processed nature of the glycans on uncleaved gp140 proteins from various genotypes including CZA97.012 attributed the finding to the use of non-lymphoid cells as a production substrate for recombinant proteins (Go et al., 2014). Our results show that this is not the explanation; BG505 SOSIP.664 trimers produced in both CHO and 293T cells bear the high-oligomannose characteristic of Env trimers derived from viruses produced in lymphoid cells (Bonomelli et al., 2011; Doores et al., 2010). Instead, we show conclusively that whether the BG505 SOSIP.664 gp140 protein is furin cleaved or not, and hence whether it does or does not adopt a native-like conformation, is the paramount factor on whether the majority of the gp120 subunit glycans remain in the oligomannose form or are processed (Figure 5). An extension to the above findings and conclusions is that the folding and oligomerization of the

furin-cleaved trimers must occur quickly enough in the Golgi apparatus to protect against significant α-mannosidase processing. Overall, the localization of furin activity and the action of Golgi α-mannosidases are critical factors that shape how the trimers are glycosylated.

The glycosylation of BG505 SOSIP.664 trimers was surprisingly homogeneous. Indeed, Ni^{2+}-affinity purification of His-tagged trimers followed by SEC was sufficient to isolate a trimer population with a native-like glycosylation profile, comparable to that achieved using bNAb-affinity columns. We caution, however, that this conclusion is highly unlikely to be generalizable to all SOSIP.664 trimer preparations based on different genotypes. In particular, if non-native, misfolded trimers are present (which is not the case with BG505), they will be co-purified with properly folded trimers when a Ni^{2+}/SEC protocol is used. In contrast, a bNAb column eliminates such unwanted contaminants, particularly when a trimer-specific bNAb such as PGT145 is used (Pugach et al., 2015).

The homogeneity of BG505 SOSIP.664 trimers has implications for developing vaccine strategies aimed at inducing glycan-dependent or glycan-avoiding bNAbs (Garces et al., 2014). Previous studies have suggested that the majority of Env glycans are highly processed (Go et al., 2014; Pabst et al., 2012). The resulting complexity could be construed to constitute a barrier against the elicitation of glycan-dependent bNAbs because the target epitope is diluted. However, the predominance of oligomannose-type glycans on all BG505 SOSIP.664 glycoforms reduces or even eliminates such concerns.

In summary, native-like BG505 SOSIP.664 trimers display a glycosylation profile dominated by oligomannose-type glycans and, in particular, large $Man_8GlcNAc_2$ and $Man_9GlcNAc_2$ structures. In contrast, uncleaved gp140s lack these key properties due to their non-native structures and the resulting loss of steric constraints on glycan-processing enzymes. Do the elevated levels of oligomannose glycans on the Env trimer have some functional role, for example, in viral tropism and in the infection process? Although we cannot answer that question yet with any certainty, we suggest that these structures arose because HIV-1 requires a high density of Env glycans to protect underlying, vulnerable, conserved protein epitopes. Oligomannose glycans may also play a role in tropism by allowing HIV-1 to interact with cell surface lectins such as DC-SIGN (Feinberg et al., 2001; Geijtenbeek et al., 2000). Irrespective of their genesis, the oligomannose components of the glycan shield constitute an Achilles' heel on the virus that can be exploited for vaccine design.

EXPERIMENTAL PROCEDURES

Env Trimer Expression and Purification

BG505 SOSIP.664 trimers were expressed in stable Flp-In 293T and CHO cells and purified by 2G12-affinity chromatography (unless stated otherwise) followed by SEC to remove monomers and dimers, as described elsewhere (Chung et al., 2014). Additionally, BG505 SOSIP.664 constructs bearing a C-terminal His-tag were expressed in 293F cells as previously described (Sanders et al., 2013). These Env proteins were purified from the culture supernatants by Ni^{2+}-NTA affinity columns, followed by SEC. The trimer fraction was then used for subsequent bNAb-affinity purifications. Affinity columns were made using a CNBr-activated Sepharose 4B resin (GE Healthcare) as previously described (Sanders et al., 2013). Antibodies used to make the affinity columns were expressed in 293F cells and purified using Protein A affinity chromatography according to the manufacturer's instructions (GE Healthcare). For bNAb-affinity purification of the trimers, the binding buffer was 500 mM NaCl, 20 mM Tris-HCl (pH 8); the wash buffer was 20 mM Tris-HCl, 500 mM NaCl (pH 8), and the trimers were eluted with 3M $MgCl_2$. The eluted trimers were immediately buffer exchanged into 10 mM Tris-HCl, 75 mM NaCl (pH 8) and concentrated using a 50 kDa cut-off Vivaspin column (GE Healthcare). A His-tagged BG505 SOSIP.664 N332A mutant was generated by site-directed mutagenesis, expressed in 293F cells, and purified by PGT151-affinity chromatography followed by SEC. Cleaved BG505 EnvΔCT trimers were expressed in 293F cells and purified by PGT151-affinity chromatography followed by SEC, as previously described (Blattner et al., 2014). Where the role of furin-cleavage was investigated, His-tagged BG505 SOSIP.664 was expressed in 293F cells with and without recombinant furin, and the resulting glycoproteins were purified by Ni^{2+}-NTA affinity chromatography. BG505 WT.SEKS uncleaved gp140 was expressed in 293T cells and purified by 2G12-affinity chromatography followed by SEC, as previously reported (Chung et al., 2014; Ringe et al., 2013; Yasmeen et al., 2014). His-tagged, uncleaved CZA97.012 gp140 was purified by Ni^{2+}-NTA affinity chromatography followed by SEC, as previously described (Chung et al., 2014; Go et al., 2014; Kovacs et al., 2012). The uncleaved CN54 gp140 (from clade C strain 97CN001, accession number GenBank: AF286226) and UG37 gp140 (from clade A strain 92/UG/037, accession number GenBank: AY494974) proteins were purchased from Polymun Scientific. These proteins are described in datasheets accessible from http://www.polymun.at and are purified using the anti-gp41 antibody 5F3, followed by ion-exchange chromatography.

Enzymatic Release of N-Linked Glycans

Env trimers (10 μg), purified in various ways, were fractionated by SDS-PAGE, with and without the addition of DTT, and the gels were stained with Coomassie blue. Bands corresponding to the gp140, gp120, or $gp41_{ECTO}$ species were excised from the gels and washed alternately with acetonitrile and water five times. N-linked glycans were then released by addition of PNGase F at 5,000 U/ml and incubation at 37°C for 16 hr, according to the manufacturer's instructions (NEB; New England Biolabs). The released glycans were subsequently eluted from gel bands by extensive washing with water and then dried using a SpeedVac concentrator.

Fluorescent Labeling of N-Linked Glycans

Released glycans were labeled with 2-AA as previously described (Neville et al., 2009). Briefly, glycans were resuspended in 30 μl of water followed by addition of 80 μl of labeling mixture (30 mg/ml 2-AA and 45 mg/ml sodium cyanoborohydride in a solution of sodium acetate trihydrate [4% w/v] and boric acid [2% w/v] in methanol). Samples were then incubated at 80°C for 1 hr. Excess label was removed using Spe-ed Amide-2 cartridges, as previously described (Neville et al., 2009).

HILIC-UPLC

Fluorescently labeled glycans were resolved by HILIC-UPLC using a 2.1 mm × 10 mm Acquity BEH Amide Column (1.7 μm particle size) (Waters). The following gradient was run: time = 0 min (t = 0): 22.0% A, 78.0% B (flow rate of 0.5 ml/min); t = 38.5: 44.1% A, 55.9% B (0.5 ml/min); t = 39.5: 100% A, 0% B (0.25 ml/min); t = 44.5: 100% A, 0% B (0.25 ml/min); t = 46.5: 22.0% A, 78.0% B (0.5 ml/min), t = 48: 22.0% A, 78.0% B (0.5 ml/min), where solvent A was 50 mM ammonium formate (pH 4.4) and solvent B was acetonitrile. Fluorescence was measured using an excitation wavelength of 250 nm and a detection wavelength of 428 nm. Data processing was performed using Empower 3 software. The percentage abundance of oligomannose-type glycans was calculated by integration of the relevant peak areas before and after Endo H digestion, following normalization.

Exoglycosidase Sequencing of N-Linked Glycans

The structures of N-linked glycans were determined by sequential digestion of labeled glycans with a panel of exoglycosidases. The enzymes used were neuraminidase from *Clostridium perfringens* (NEB), α-L-fucosidase from bovine kidney (Sigma), β1,4-galactosidase from *Streptococcus pneumoniae*, β-*N*-acetylglucosaminidase from *S. pneumonia*, and α(1-2,3,6)-mannosidase

from Jack bean (QA Bio). Endoglycosidase H (NEB) was used for quantitation of oligomannose structures. Digestions were performed at 37°C for 16 hr, according to manufacturers' instructions. The digested glycans were purified using a polyvinylidene fluoride (PVDF) protein-binding membrane plate (Millipore) prior to HILIC-UPLC analysis.

Negative Stain EM

Env proteins were prepared for negative stain EM analysis as previously described (Pugach et al., 2015; Ringe et al., 2013; Sanders et al., 2013). Briefly, a 3 μl aliquot containing ~0.03 mg/ml of Env protein was applied for 5 s onto a carbon-coated 400 Cu mesh grid that had been glow discharged at 20 mA for 30 s and then negatively stained with 2% (w/v) uranyl formate for 60 s. Data were collected using an FEI Tecnai T12 electron microscope operating at 120 keV, with an electron dose of ~25 e^{-}/Å^2 and a magnification of 52,000× that resulted in a pixel size of 2.05 Å at the specimen plane. Images were acquired with a Tietz TemCam-F416 CMOS camera using a nominal defocus range of 1000 nm.

Data processing methods were adapted from those used previously (Pugach et al., 2015; Ringe et al., 2013; Sanders et al., 2013). In summary, the Appion software package (Voss et al., 2009) was used to automatically pick particles, create stacks, and calculate reference-free 2D class averages with iterative MSA/MRA (Ogura et al., 2003). The 2D class averages were visually inspected and the classes were segregated into one of three structural groups labeled "closed," "open," or "non-native" as described previously (Pugach et al., 2015). The amount of native-like particles was defined as the sum of "closed" and "open" particles.

SUPPLEMENTAL INFORMATION

Supplemental Information includes four figures and two tables and can be found with this article online at http://dx.doi.org/10.1016/j.celrep.2015.05.017.

AUTHOR CONTRIBUTIONS

L.K.P., S.V., G.O., G.E.S., H.J.K., and A.C. performed experimental work. L.K.P., S.V., G.O., R.W.S., K.J.D., D.R.B., I.A.W., A.B.W., J.P.M., and M.C. analyzed data. L.K.P., G.O., K.J.D., R.W.S., D.R.B., I.A.W., A.B.W., J.P.M., and M.C. wrote the paper. J.P.M. and M.C. designed the study. All authors read and approved the final manuscript.

ACKNOWLEDGMENTS

We dedicate this article in memory of our good friend and greatly admired colleague, Dr. Chris Scanlan. The CN54 gp140 and UG37 gp140 proteins were kindly provided by Professor Quentin Sattentau (University of Oxford). We thank Professor Raymond A. Dwek FRS for constant unwavering support and insightful discussions. L.K.P. was supported by a Scholarship from the Department of Biochemistry, University of Oxford. M.C. is a Fellow of Oriel College, Oxford. This work was supported by NIH HIVRAD grant P01 AI082362, an International AIDS Vaccine Initiative Neutralizing Antibody Center CAVD grant (Glycan characterization and Outer Domain glycoform design), the Scripps CHAVI-ID (1UM1AI100663), and the Medical Research Council MR/K024426/1. R.W.S. is a recipient of a Vidi grant from the Netherlands Organization for Scientific Research (NWO) and a Starting Investigator Grant from the European Research Council (ERC-StG-2011–280829-SHEV). J.P.M., R.W.S., A.B.W., I.A.W., and A.C. are listed as inventors on patent applications relating to the general use of BG505 SOSIP.664 trimers and/or their production in stable CHO and 293T cell lines.

Received: December 2, 2014
Revised: April 23, 2015
Accepted: May 11, 2015
Published: June 4, 2015

REFERENCES

Blattner, C., Lee, J.H., Sliepen, K., Derking, R., Falkowska, E., de la Peña, A.T., Cupo, A., Julien, J.-P., van Gils, M., Lee, P.S., et al. (2014). Structural delineation of a quaternary, cleavage-dependent epitope at the gp41-gp120 interface on intact HIV-1 Env trimers. Immunity *40*, 669–680.

Bonomelli, C., Doores, K.J., Dunlop, D.C., Thaney, V., Dwek, R.A., Burton, D.R., Crispin, M., and Scanlan, C.N. (2011). The glycan shield of HIV is predominantly oligomannose independently of production system or viral clade. PLoS ONE *6*, e23521.

Burton, D.R., Ahmed, R., Barouch, D.H., Butera, S.T., Crotty, S., Godzik, A., Kaufmann, D.E., McElrath, M.J., Nussenzweig, M.C., Pulendran, B., et al. (2012). A blueprint for HIV vaccine discovery. Cell Host Microbe *12*, 396–407.

Calarese, D.A., Scanlan, C.N., Zwick, M.B., Deechongkit, S., Mimura, Y., Kunert, R., Zhu, P., Wormald, M.R., Stanfield, R.L., Roux, K.H., et al. (2003). Antibody domain exchange is an immunological solution to carbohydrate cluster recognition. Science *300*, 2065–2071.

Chung, N.P., Matthews, K., Kim, H.J., Ketas, T.J., Golabek, M., de Los Reyes, K., Korzun, J., Yasmeen, A., Sanders, R.W., Klasse, P.J., et al. (2014). Stable 293 T and CHO cell lines expressing cleaved, stable HIV-1 envelope glycoprotein trimers for structural and vaccine studies. Retrovirology *11*, 33.

Crispin, M., and Bowden, T.A. (2013). Antibodies expose multiple weaknesses in the glycan shield of HIV. Nat. Struct. Mol. Biol. *20*, 771–772.

Crooks, E.T., Tong, T., Osawa, K., and Binley, J.M. (2011). Enzyme digests eliminate nonfunctional Env from HIV-1 particle surfaces, leaving native Env trimers intact and viral infectivity unaffected. J. Virol. *85*, 5825–5839.

Doores, K.J., Bonomelli, C., Harvey, D.J., Vasiljevic, S., Dwek, R.A., Burton, D.R., Crispin, M., and Scanlan, C.N. (2010). Envelope glycans of immunodeficiency virions are almost entirely oligomannose antigens. Proc. Natl. Acad. Sci. USA *107*, 13800–13805.

Dunlop, D.C., Bonomelli, C., Mansab, F., Vasiljevic, S., Doores, K.J., Wormald, M.R., Palma, A.S., Feizi, T., Harvey, D.J., Dwek, R.A., et al. (2010). Polysaccharide mimicry of the epitope of the broadly neutralizing anti-HIV antibody, 2G12, induces enhanced antibody responses to self oligomannose glycans. Glycobiology *20*, 812–823.

Falkowska, E., Le, K.M., Ramos, A., Doores, K.J., Lee, J.H., Blattner, C., Ramirez, A., Derking, R., van Gils, M.J., Liang, C.-H., et al. (2014). Broadly neutralizing HIV antibodies define a glycan-dependent epitope on the prefusion conformation of gp41 on cleaved envelope trimers. Immunity *40*, 657–668.

Feinberg, H., Mitchell, D.A., Drickamer, K., and Weis, W.I. (2001). Structural basis for selective recognition of oligosaccharides by DC-SIGN and DC-SIGNR. Science *294*, 2163–2166.

Garces, F., Sok, D., Kong, L., McBride, R., Kim, H.J., Saye-Francisco, K.F., Julien, J.-P., Hua, Y., Cupo, A., Moore, J.P., et al. (2014). Structural evolution of glycan recognition by a family of potent HIV antibodies. Cell *159*, 69–79.

Geijtenbeek, T.B., Torensma, R., van Vliet, S.J., van Duijnhoven, G.C., Adema, G.J., van Kooyk, Y., and Figdor, C.G. (2000). Identification of DC-SIGN, a novel dendritic cell-specific ICAM-3 receptor that supports primary immune responses. Cell *100*, 575–585.

Georgiev, I.S., Joyce, M.G., Yang, Y., Sastry, M., Zhang, B., Baxa, U., Chen, R.E., Druz, A., Lees, C.R., Narpala, S., et al. (2015). Single-chain soluble BG505.SOSIP gp140 trimers as structural and antigenic mimics of mature closed HIV-1. Env. J. Virol. *89*, 5318–5329.

Go, E.P., Liao, H.-X., Alam, S.M., Hua, D., Haynes, B.F., and Desaire, H. (2013). Characterization of host-cell line specific glycosylation profiles of early transmitted/founder HIV-1 gp120 envelope proteins. J. Proteome Res. *12*, 1223–1234.

Go, E.P., Hua, D., and Desaire, H. (2014). Glycosylation and disulfide bond analysis of transiently and stably expressed clade C HIV-1 gp140 trimers in 293T cells identifies disulfide heterogeneity present in both proteins and differences in O-linked glycosylation. J. Proteome Res. *13*, 4012–4027.

Guttman, M., Garcia, N.K., Cupo, A., Matsui, T., Julien, J.-P., Sanders, R.W., Wilson, I.A., Moore, J.P., and Lee, K.K. (2014). CD4-induced activation in a soluble HIV-1 Env trimer. Structure *22*, 974–984.

Hessell, A.J., Rakasz, E.G., Poignard, P., Hangartner, L., Landucci, G., Forthal, D.N., Koff, W.C., Watkins, D.I., and Burton, D.R. (2009). Broadly neutralizing human anti-HIV antibody 2G12 is effective in protection against mucosal

SHIV challenge even at low serum neutralizing titers. PLoS Pathog. *5*, e1000433.

Huang, J., Kang, B.H., Pancera, M., Lee, J.H., Tong, T., Feng, Y., Imamichi, H., Georgiev, I.S., Chuang, G.Y., Druz, A., et al. (2014). Broad and potent HIV-1 neutralization by a human antibody that binds the gp41-gp120 interface. Nature *515*, 138–142.

Julien, J.-P., Cupo, A., Sok, D., Stanfield, R.L., Lyumkis, D., Deller, M.C., Klasse, P.-J., Burton, D.R., Sanders, R.W., Moore, J.P., et al. (2013). Crystal structure of a soluble cleaved HIV-1 envelope trimer. Science *342*, 1477–1483.

Kong, L., Lee, J.H., Doores, K.J., Murin, C.D., Julien, J.P., McBride, R., Liu, Y., Marozsan, A., Cupo, A., Klasse, P.J., et al. (2013). Supersite of immune vulnerability on the glycosylated face of HIV-1 envelope glycoprotein gp120. Nat. Struct. Mol. Biol. *20*, 796–803.

Kovacs, J.M., Nkolola, J.P., Peng, H., Cheung, A., Perry, J., Miller, C.A., Seaman, M.S., Barouch, D.H., and Chen, B. (2012). HIV-1 envelope trimer elicits more potent neutralizing antibody responses than monomeric gp120. Proc. Natl. Acad. Sci. USA *109*, 12111–12116.

Lasky, L.A., Groopman, J.E., Fennie, C.W., Benz, P.M., Capon, D.J., Dowbenko, D.J., Nakamura, G.R., Nunes, W.M., Renz, M.E., and Berman, P.W. (1986). Neutralization of the AIDS retrovirus by antibodies to a recombinant envelope glycoprotein. Science *233*, 209–212.

Leonard, C.K., Spellman, M.W., Riddle, L., Harris, R.J., Thomas, J.N., and Gregory, T.J. (1990). Assignment of intrachain disulfide bonds and characterization of potential glycosylation sites of the type 1 recombinant human immunodeficiency virus envelope glycoprotein (gp120) expressed in Chinese hamster ovary cells. J. Biol. Chem. *265*, 10373–10382.

Lewis, D.J., Fraser, C.A., Mahmoud, A.N., Wiggins, R.C., Woodrow, M., Cope, A., Cai, C., Giemza, R., Jeffs, S.A., Manoussaka, M., et al. (2011). Phase I randomised clinical trial of an HIV-1(CN54), clade C, trimeric envelope vaccine candidate delivered vaginally. PLoS ONE *6*, e25165.

Lewis, D.J.M., Wang, Y., Huo, Z., Giemza, R., Babaahmady, K., Rahman, D., Shattock, R.J., Singh, M., and Lehner, T. (2014). Effect of vaginal immunization with HIVgp140 and HSP70 on HIV-1 replication and innate and T cell adaptive immunity in women. J. Virol. *88*, 11648–11657.

Liu, J., Bartesaghi, A., Borgnia, M.J., Sapiro, G., and Subramaniam, S. (2008). Molecular architecture of native HIV-1 gp120 trimers. Nature *455*, 109–113.

Lyumkis, D., Julien, J.-P., de Val, N., Cupo, A., Potter, C.S., Klasse, P.-J., Burton, D.R., Sanders, R.W., Moore, J.P., Carragher, B., et al. (2013). Cryo-EM structure of a fully glycosylated soluble cleaved HIV-1 envelope trimer. Science *342*, 1484–1490.

Mascola, J.R., Stiegler, G., VanCott, T.C., Katinger, H., Carpenter, C.B., Hanson, C.E., Beary, H., Hayes, D., Frankel, S.S., Birx, D.L., and Lewis, M.G. (2000). Protection of macaques against vaginal transmission of a pathogenic HIV-1/SIV chimeric virus by passive infusion of neutralizing antibodies. Nat. Med. *6*, 207–210.

McLellan, J.S., Pancera, M., Carrico, C., Gorman, J., Julien, J.-P., Khayat, R., Louder, R., Pejchal, R., Sastry, M., Dai, K., et al. (2011). Structure of HIV-1 gp120 V1/V2 domain with broadly neutralizing antibody PG9. Nature *480*, 336–343.

Moldt, B., Rakasz, E.G., Schultz, N., Chan-Hui, P.-Y., Swiderek, K., Weisgrau, K.L., Piaskowski, S.M., Bergman, Z., Watkins, D.I., Poignard, P., and Burton, D.R. (2012). Highly potent HIV-specific antibody neutralization in vitro translates into effective protection against mucosal SHIV challenge in vivo. Proc. Natl. Acad. Sci. USA *109*, 18921–18925.

Moscoso, C.G., Xing, L., Hui, J., Hu, J., Kalkhoran, M.B., Yenigun, O.M., Sun, Y., Paavolainen, L., Martin, L., Vahlne, A., et al. (2014). Trimeric HIV Env provides epitope occlusion mediated by hypervariable loops. Sci. Rep. *4*, 7025.

Mouquet, H., Scharf, L., Euler, Z., Liu, Y., Eden, C., Scheid, J.F., Halper-Stromberg, A., Gnanapragasam, P.N.P., Spencer, D.I.R., Seaman, M.S., et al. (2012). Complex-type N-glycan recognition by potent broadly neutralizing HIV antibodies. Proc. Natl. Acad. Sci. USA *109*, E3268–E3277.

Murin, C.D., Julien, J.-P., Sok, D., Stanfield, R.L., Khayat, R., Cupo, A., Moore, J.P., Burton, D.R., Wilson, I.A., and Ward, A.B. (2014). Structure of 2G12 Fab2 in complex with soluble and fully glycosylated HIV-1 Env by negative-stain single-particle electron microscopy. J. Virol. *88*, 10177–10188.

Neville, D.C.A., Dwek, R.A., and Butters, T.D. (2009). Development of a single column method for the separation of lipid- and protein-derived oligosaccharides. J. Proteome Res. *8*, 681–687.

Nkolola, J.P., Peng, H., Settembre, E.C., Freeman, M., Grandpre, L.E., Devoy, C., Lynch, D.M., La Porte, A., Simmons, N.L., Bradley, R., et al. (2010). Breadth of neutralizing antibodies elicited by stable, homogeneous clade A and clade C HIV-1 gp140 envelope trimers in guinea pigs. J. Virol. *84*, 3270–3279.

Ogura, T., Iwasaki, K., and Sato, C. (2003). Topology representing network enables highly accurate classification of protein images taken by cryo electron-microscope without masking. J. Struct. Biol. *143*, 185–200.

Pabst, M., Chang, M., Stadlmann, J., and Altmann, F. (2012). Glycan profiles of the 27 N-glycosylation sites of the HIV envelope protein CN54gp140. Biol. Chem. *393*, 719–730.

Pancera, M., Shahzad-Ul-Hussan, S., Doria-Rose, N.A., McLellan, J.S., Bailer, R.T., Dai, K., Loesgen, S., Louder, M.K., Staupe, R.P., Yang, Y., et al. (2013). Structural basis for diverse N-glycan recognition by HIV-1-neutralizing V1-V2-directed antibody PG16. Nat. Struct. Mol. Biol. *20*, 804–813.

Pancera, M., Zhou, T., Druz, A., Georgiev, I.S., Soto, C., Gorman, J., Huang, J., Acharya, P., Chuang, G.-Y., Ofek, G., et al. (2014). Structure and immune recognition of trimeric pre-fusion HIV-1 Env. Nature *514*, 455–461.

Pejchal, R., Doores, K.J., Walker, L.M., Khayat, R., Huang, P.-S., Wang, S.-K., Stanfield, R.L., Julien, J.-P., Ramos, A., Crispin, M., et al. (2011). A potent and broad neutralizing antibody recognizes and penetrates the HIV glycan shield. Science *334*, 1097–1103.

Pugach, P., Ozorowski, G., Cupo, A., Ringe, R., Yasmeen, A., de Val, N., Derking, R., Kim, H.J., Korzun, J., Golabek, M., et al. (2015). A native-like SOSIP.664 trimer based on an HIV-1 subtype B env gene. J. Virol. *89*, 3380–3395.

Raska, M., Takahashi, K., Czernekova, L., Zachova, K., Hall, S., Moldoveanu, Z., Elliott, M.C., Wilson, L., Brown, R., Jancova, D., et al. (2010). Glycosylation patterns of HIV-1 gp120 depend on the type of expressing cells and affect antibody recognition. J. Biol. Chem. *285*, 20860–20869.

Ringe, R.P., Sanders, R.W., Yasmeen, A., Kim, H.J., Lee, J.H., Cupo, A., Korzun, J., Derking, R., van Montfort, T., Julien, J.P., et al. (2013). Cleavage strongly influences whether soluble HIV-1 envelope glycoprotein trimers adopt a native-like conformation. Proc. Natl. Acad. Sci. USA *110*, 18256–18261.

Sanders, R.W., Venturi, M., Schiffner, L., Kalyanaraman, R., Katinger, H., Lloyd, K.O., Kwong, P.D., and Moore, J.P. (2002). The mannose-dependent epitope for neutralizing antibody 2G12 on human immunodeficiency virus type 1 glycoprotein gp120. J. Virol. *76*, 7293–7305.

Sanders, R.W., Derking, R., Cupo, A., Julien, J.-P., Yasmeen, A., de Val, N., Kim, H.J., Blattner, C., de la Peña, A.T., Korzun, J., et al. (2013). A next-generation cleaved, soluble HIV-1 Env trimer, BG505 SOSIP.664 gp140, expresses multiple epitopes for broadly neutralizing but not non-neutralizing antibodies. PLoS Pathog. *9*, e1003618.

Scanlan, C.N., Pantophlet, R., Wormald, M.R., Ollmann Saphire, E., Stanfield, R., Wilson, I.A., Katinger, H., Dwek, R.A., Rudd, P.M., and Burton, D.R. (2002). The broadly neutralizing anti-human immunodeficiency virus type 1 antibody 2G12 recognizes a cluster of α1−>2 mannose residues on the outer face of gp120. J. Virol. *76*, 7306–7321.

Scharf, L., Scheid, J.F., Lee, J.H., West, A.P., Jr., Chen, C., Gao, H., Gnanapragasam, P.N.P., Mares, R., Seaman, M.S., Ward, A.B., et al. (2014). Antibody 8ANC195 reveals a site of broad vulnerability on the HIV-1 envelope spike. Cell Rep. *7*, 785–795.

Schiffner, T., Kong, L., Duncan, C.J., Back, J.W., Benschop, J.J., Shen, X., Huang, P.S., Stewart-Jones, G.B., DeStefano, J., Seaman, M.S., et al. (2013). Immune focusing and enhanced neutralization induced by HIV-1 gp140 chemical cross-linking. J. Virol. *87*, 10163–10172.

Tran, K., Poulsen, C., Guenaga, J., de Val, N., Wilson, R., Sundling, C., Li, Y., Stanfield, R.L., Wilson, I.A., Ward, A.B., et al. (2014). Vaccine-elicited primate antibodies use a distinct approach to the HIV-1 primary receptor binding site informing vaccine redesign. Proc. Natl. Acad. Sci. USA *111*, E738–E747.

Voss, N.R., Yoshioka, C.K., Radermacher, M., Potter, C.S., and Carragher, B. (2009). DoG Picker and TiltPicker: software tools to facilitate particle selection in single particle electron microscopy. J. Struct. Biol. *166*, 205–213.

Walker, L.M., Phogat, S.K., Chan-Hui, P.-Y., Wagner, D., Phung, P., Goss, J.L., Wrin, T., Simek, M.D., Fling, S., Mitcham, J.L., et al.; Protocol G Principal Investigators (2009). Broad and potent neutralizing antibodies from an African donor reveal a new HIV-1 vaccine target. Science *326*, 285–289.

Walker, L.M., Huber, M., Doores, K.J., Falkowska, E., Pejchal, R., Julien, J.-P., Wang, S.-K., Ramos, A., Chan-Hui, P.-Y., Moyle, M., et al.; Protocol G Principal Investigators (2011). Broad neutralization coverage of HIV by multiple highly potent antibodies. Nature *477*, 466–470.

Yasmeen, A., Ringe, R., Derking, R., Cupo, A., Julien, J.-P., Burton, D.R., Ward, A.B., Wilson, I.A., Sanders, R.W., Moore, J.P., and Klasse, P.J. (2014). Differential binding of neutralizing and non-neutralizing antibodies to native-like soluble HIV-1 Env trimers, uncleaved Env proteins, and monomeric subunits. Retrovirology *11*, 41.